Giant electric-field induced thermal switching controlled by phonon scattering in a relaxor ferroelectric
Supplementary Information

Puspa Upreti[1*†], Delaram Rashadfar[2†], Raffi Sahul[3], Douglas L. Abernathy[4], Joseph P. Heremans[5,6], Raphaël P. Hermann[1], Michael E. Manley[1*]

[1*]Materials Science and Technology Division, Oak Ridge National Laboratory, Oak Ridge, 37831, Tennessee, USA.
[2]Department of Mechanical and Aerospace Engineering, Ohio State University, Columbus, 43210, Ohio, USA.
[3]Amphenol Corporation, 21701, Maryland, USA.
[4]Neutron Science Division, Oak Ridge National Laboratory, Oak Ridge, 37831, Tennessee, USA.
[5]Department of Material Science and Aerospace Engineering, Ohio State University, Columbus, 43210, Ohio, USA.
[6]Department of Physics, Ohio State University, Columbus, 43210, Ohio, USA.

*Corresponding author(s). E-mail(s): upretipr@ornl.gov; manleyme@ornl.gov;
†These authors contributed equally to this work.

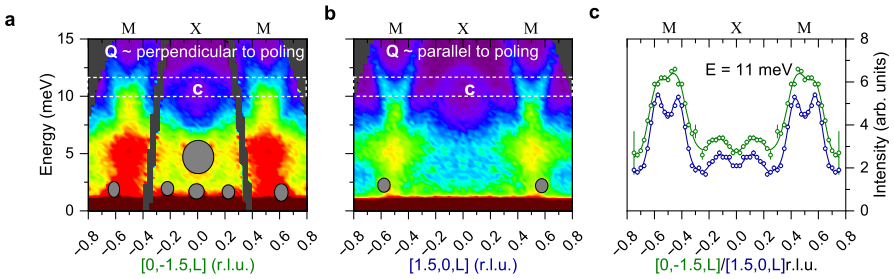

Fig. S1: **Poling effects along the zone boundary along M to X points in PMN-30%PT.** (**a**) Phonon dispersion measured along $\mathbf{Q} = [0, -1.5, L]$. (**b**) Phonon dispersion measured along $\mathbf{Q} = [1.5, 0, L]$. The grey circles in (**a**) and (**b**) are the artifacts in the scattering. (**c**) Fits to the corresponding cuts through the data in (**a**) and (**b**) with intensities integrated in E from 10 to 12 meV and $\Delta q = \pm 0.05$ r.l.u. in orthogonal direction to L axis shown as white dashed rectangular boxes in (**a**) and (**b**). Scattering vector in (**a**) is perpendicular to poling direction where as that is parallel to poling axis in **b**. All the phonon modes appear broad in the direction perpendicular to poling and relatively sharp along the poling axis. Also seen the unusual strong softening of zone-boundary modes at M-points down to elastic line for **Q** perpendicular to poling (**a**).

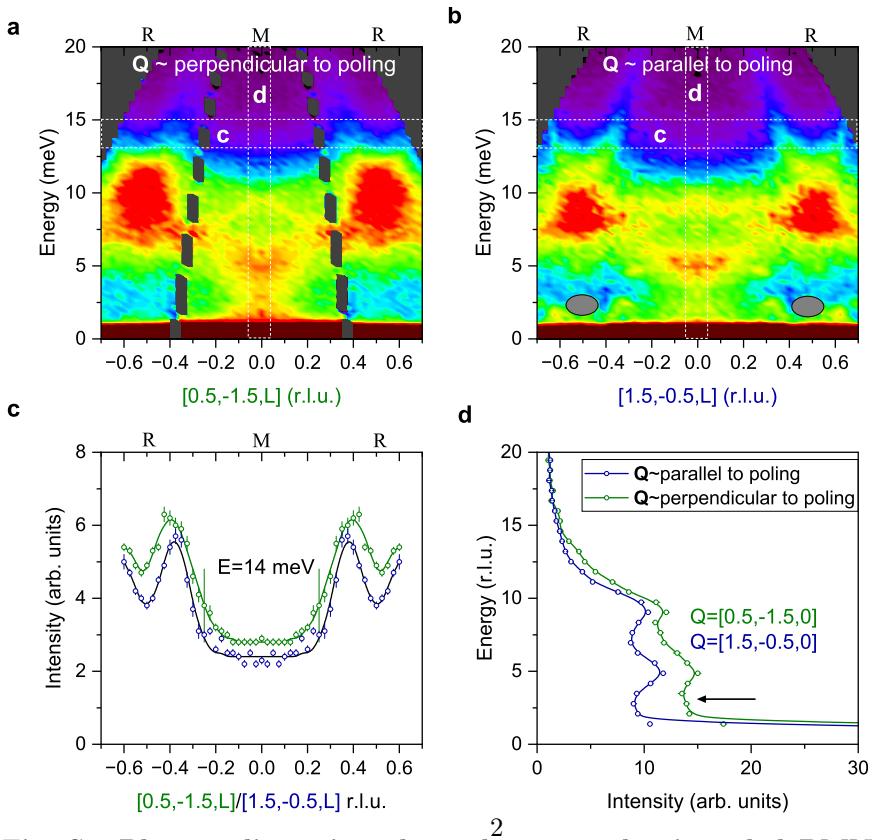

Fig. S2: **Phonon dispersion along the zone edge in poled PMN-30%PT.** (**a**) Phonon dispersion measured along $\mathbf{Q} = [0.5, -1.5, L]$ perpendicular to poling direction. (**b**) Phonon dispersion measured along $\mathbf{Q} = [1.5, -0.5, L]$ parallel to poling direction. (**c**) Fits to the corresponding cuts through the data in (**a**) and (**b**) with intensities integrated in E from 13 to 15 meV and $\Delta q = \pm 0.05$ r.l.u. in orthogonal direction to L axis shown as white dashed horizontal rectangular boxes in (**a**) and (**b**). (**d**) Inelastic scattering intensity at $L = 0$ in (**a**) and (**b**) with integration of $\Delta q = \pm 0.05$ r.l.u. along all H, K, and L (white dashed vertical rectangular boxes) showing marked antiferroelectric fluctuations extending down to elastic line for scattering vector perpendicular to poling direction. All the phonon modes have relatively broad linewidths compared to those modes along the poling direction.

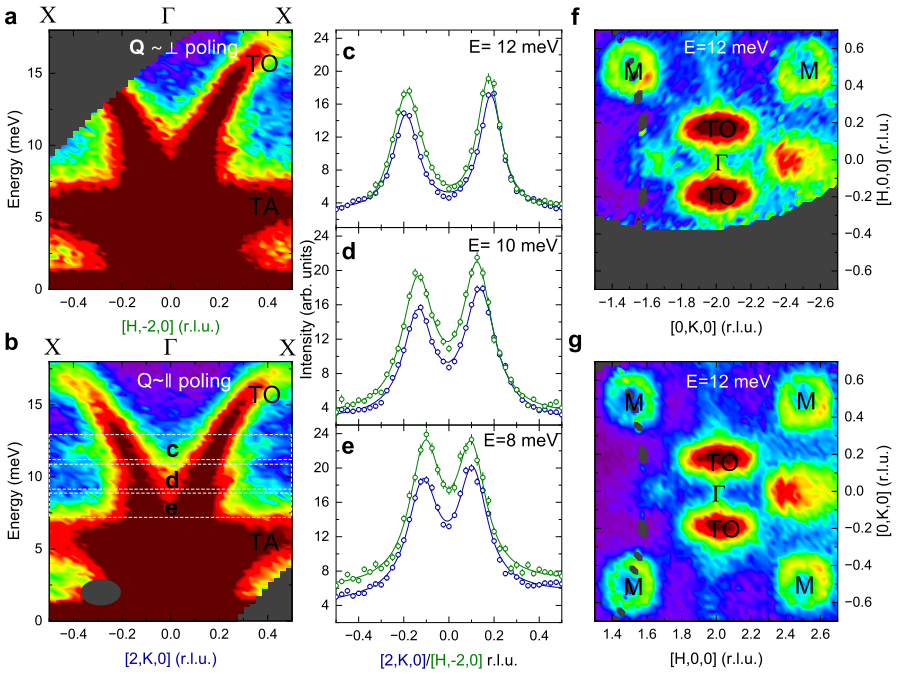

Fig. S3: **Transverse phonon dispersions in [100]-poled PMN-30%PT along zone centers in two unique directions.** (**a**) and (**b**) Transverse phonon dispersion measured respectively along $\mathbf{Q} = [H, -2, 0]$ and $\mathbf{Q} = [2, K, 0]$. (**c**), (**d**), (**e**) Fits to one dimension cuts at energies 12, 10 and 8 meV respectively with integration, $\Delta E = \pm 1$ meV, in E and $\Delta q = \pm 0.05$ r.l.u. in orthogonal direction to L axis along both $\mathbf{Q} = [H, -2, 0]$ (green) and $\mathbf{Q} = [2, K, 0]$ (blue). (**f**) and (**g**) Constant energy slice at 12 meV taken in $(H,K,0)$ planes. In (**a**) and (**f**) scattering vectors are perpendicular to poling axis whereas in (**b**) and (**g**), by contrast, have scattering vectors along the poling axis. All the phonons are broad in the case of atomic displacements perpendicular to the poling direction (**a** and **f**) and relatively sharp for displacements along the poling axis (**b** and **g**). It is also reported in our previous work [1] that TO mode when $\mathbf{Q} \parallel$ poling rises due to the PNR mode present roughly at 12 meV present in this direction (**b**) and as observed shift in peak position in that direction (**c**-**e**).

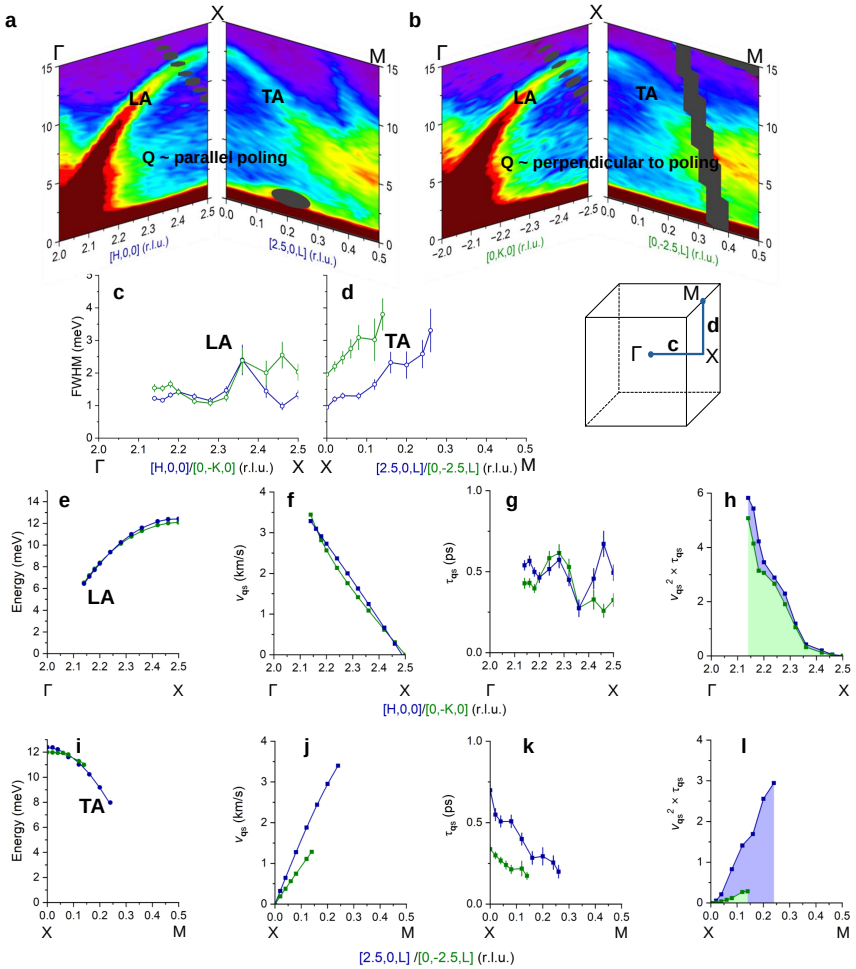

Fig. S4: **Poling effect on the phonon thermal transport in PMN-30%PT.** (**a**) and (**b**) Phonon dispersions measured along zone centers from Γ to **X** to **M** in the direction parallel and perpendicular to poling respectively. (**c**) and (**d**) show FWHM of the LA and TA modes along directions parallel and perpendicular direction to poling, respectively. (**e-h**) Breakdown of the [H,0,0]-LA phonon and [0,-K,0]-LA phonon contributions to the thermal conductivity along [100] and [010] directions. (**e**) Analytical curves fit to the measured TA phonon. (**f**) Group velocities of LA-phonon,$v_{\mathbf{q}s} = dE/dq$, in km/s. (**g**) Lifetimes of LA phonon $\tau_{qs} = \hbar/FWHM$, in ps. (**h**) Product of $\mathrm{v}^2_{\mathbf{q}s}$ and phonon lifetime ($\tau_{\mathbf{q}s}$) reveals the relative contribution of the [H,0,0]-LA phonon and [0,-K,0]-LA phonon to the thermal conductivity along [100] and [010] directions respectively (area under the curves). Likewise, (**i-l**) breakdown of the [2.5,0,L]-TA phonon and [0,-2.5,L]-TA phonon contributions to the thermal conductivity along [100] and [010] directions. The relative contribution of the [2.5,0,L]-TA phonon (area under the blue curve) to the κ is significantly higher than that of the [0,-2.5,L]-TA phonon (area under the green curve).

Fig. S4 quantitatively illuminates the mode-specific contributions to the poling effect on phonon thermal transport. The contributing parameters to phonon thermal conductivity (Eq. 1 in main article)—mode specific heat capacity (C_{qs}), phonon group velocity (v_{qs}) and phonon lifetimes (τ_{qs})—can be derived from the phonon dispersion curve [2, 3]. In the high temperature limit, the heat capacity is proportional to the density of states ($D_s(E)$) [3]. Since poling has a minimal effect on the dispersion of the LA/TA modes in both directions (Fig. S4**e,i**), this implies less impact on the phonon group velocities ($v_{qs} = dE/dq$), and also on $D_s(E)$ ($D_s(E) \propto q^2(E)(dq/dE)$). However, significant sharpening of the TA modes along the poling axis, compared to those perpendicular to the poling axis, indicates longer phonon lifetimes ($\tau_{qs} = \hbar/FWHM$) in that direction (see Fig. S4**d**,**k**). From Fig. S4**l** we can speculate that the combined effect of $v^2_{\mathbf{q}s}\tau_{\mathbf{q}s}$ is approximately six times greater along the poling direction if the green curve is extrapolated to $L = 0.24$.

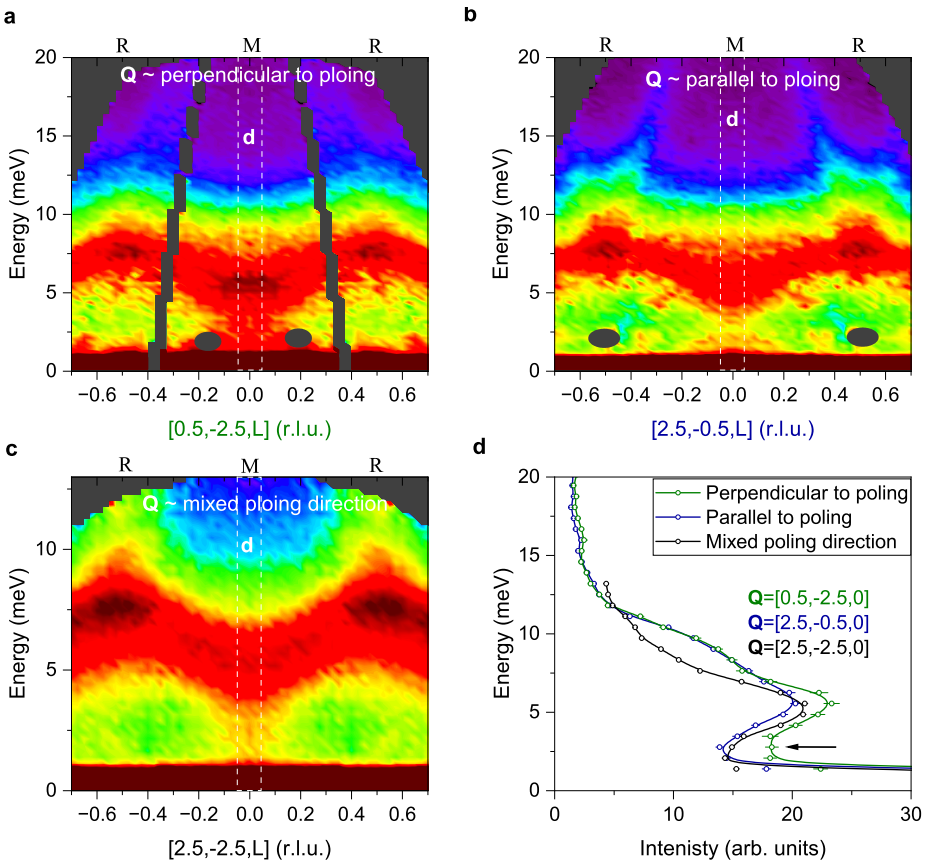

Fig. S5: **Phonon dispersion comparison along zone edge perpendicular, parallel and in between the poling directions.** (**a**) Phonon dispersion measured along $\mathbf{Q} = [0.5, -2.5, L]$ perpendicular to poling direction. (**b**) Phonon dispersion measured along $\mathbf{Q} = [2.5, -0.5, L]$ parallel to poling direction. (**c**) Phonon dispersion measured along $\mathbf{Q} = [2.5, -2.5, L]$ at mixed poling direction. (**d**) Inelastic scattering intensity at $L = 0$ in (**a**), (**b**) and (**c**) with integration of $\Delta q = \pm 0.05$ r.l.u. along all H, K, and L (white dashed vertical rectangular boxes) showing marked antiferroelectric fluctuations extending down to elastic line for scattering vector perpendicular to poling direction (black arrow in (**d**)). The mode in mixed poling direction also shows the continuum of scattering over energy transfers at zone-boundary M points down to elastic line but relatively weaker than in perpendicular direction.

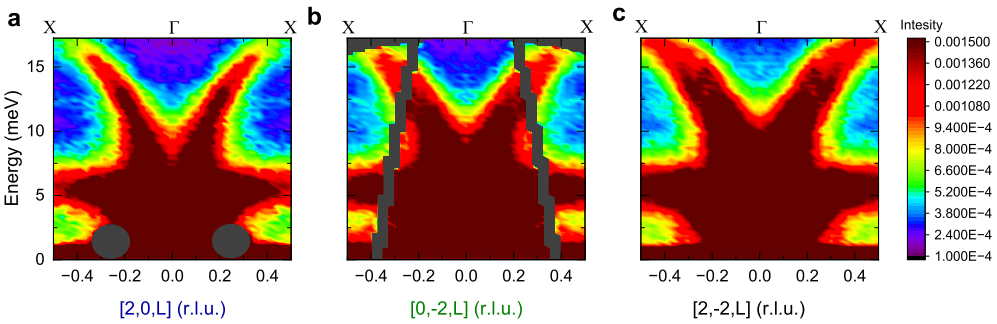

Fig. S6: **Phonon dispersion comparison along zone center perpendicular, parallel and in between the poling directions.** (**a**) Phonon dispersion measured along $\mathbf{Q} = [2, 0, L]$ parallel to the poling direction. (**b**) Phonon dispersion measured along $\mathbf{Q} = [0, -2, L]$ perpendicular to the poling direction. (**c**) Phonon dispersion measured along $\mathbf{Q} = [2, -2, L]$ at mixed poling direction.

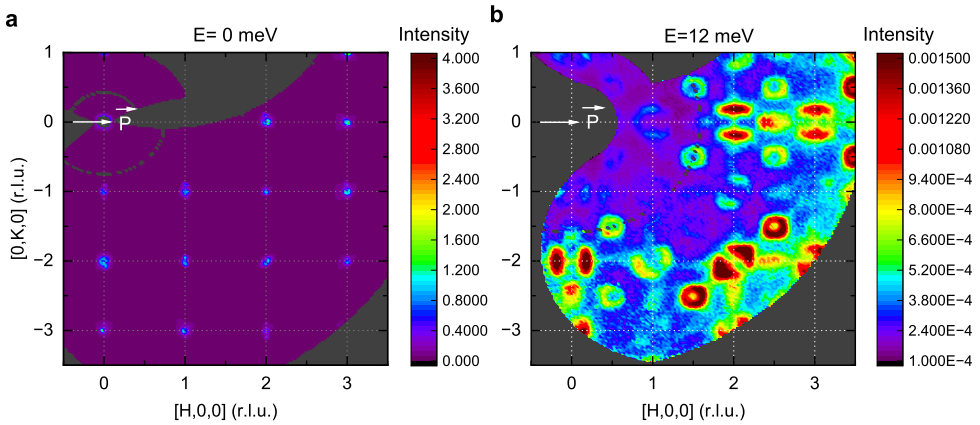

Fig. S7: **Phonon spectrum in [100]-poled PMN-30%PT.** Braggs plane at constant energy at $E = 0$ meV in (HK0) plane (**a**) showing the perfection of single crystal in our experiment and an overview of phonon modes (**b**) at constant energy slice at $E = 12$ meV in (HK0) plane.

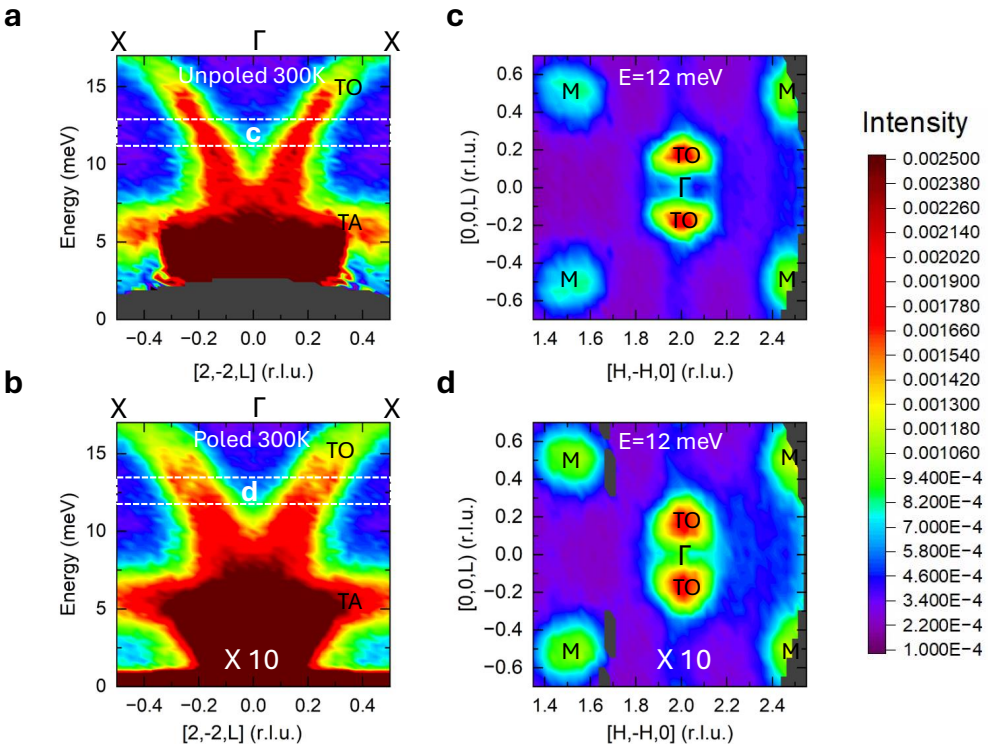

Fig. S8: **Comparing phonon dispersion in unpoled and [100]-poled PMN-30%PT.** (**a**) and (**b**) Transverse phonon dispersion measured along $\mathbf{Q} = [2, -2, L]$ respectively for unpoled and poled crystal at 300 K. (**c**) and (**d**) Constant energy slices at 12 meV taken in (*H*,-*H*,*L*) planes in both poled and unpoled cases. The intensities for poled case are scaled by factors shown in (**b**) and (**d**). The phonons are significantly broad when poled. It is also observed that the "waterfall" regime in TO branch ($0 < L <\approx \pm 0.25$ r.l.u.) along this [2,-2,L] mode remains unaffected by poling.

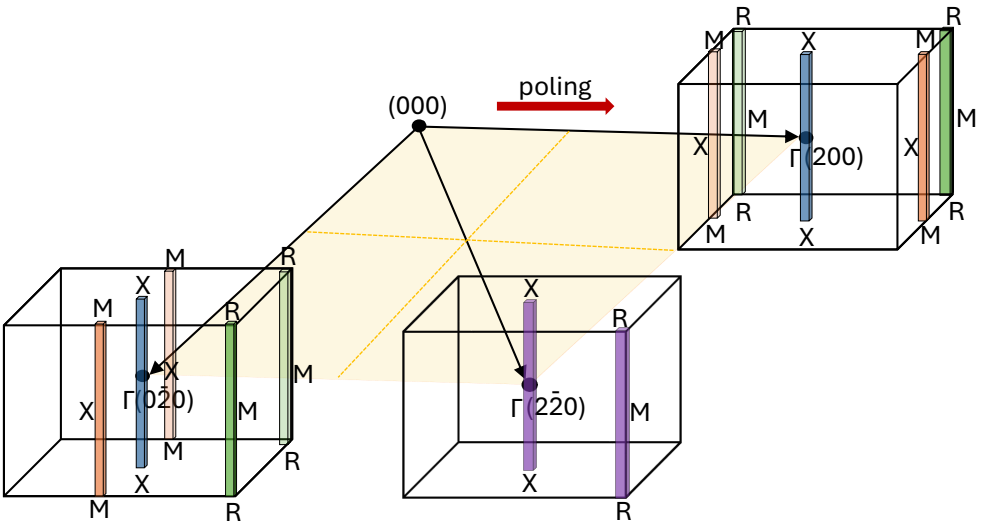

Fig. S9: **Schematic representation of the phonon modes used in the text.** All the modes are transverse. Dark blue rods represent Figs. 2**a**,**b**, dark orange rods represent Figs. 2**h**,**i** and dark green rods represent Fig. 3 respectively of the main article. Light orange and light green rods represent Figs. S1, and S2 respectively. Solid purple rods represent Figs. S5**c** and S6**c**.

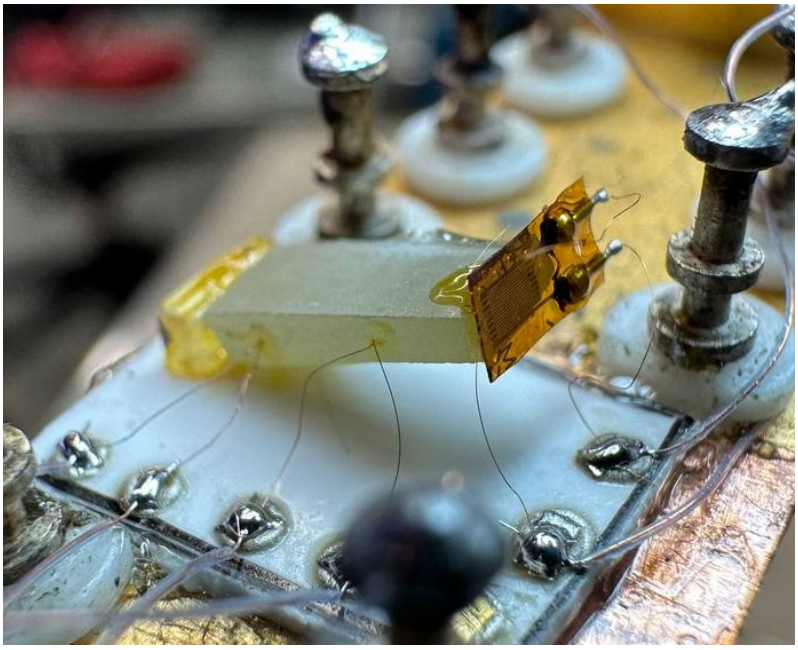

Fig. S10: **Sample mount for thermal conductivity measurement in [100]-poled PMN-30%PT.** Two thermocouples are attached to the sample using GE varnish, with a strain gauge on top acting as a heater. Heat flows from the heater down to the LiF and alumina base, which serves as the heat sink. All components were fixed in place using GE varnish.

References

[1] Manley, M. E. *et al.* Giant electromechanical coupling of relaxor ferroelectrics controlled by polar nanoregion vibrations. *Science Advances* **2**, e1501814 (2016).

[2] Manley, M. E. *et al.* Phason-dominated thermal transport in fresnoite. *Phys. Rev. Lett.* **129**, 255901 (2022).

[3] Manley, M. E. *et al.* Supersonic propagation of lattice energy by phasons in fresnoite. *Nature Communications* **9**, 1823 (2018).